Journal of Solid Mechanics Vol. 4, No. 3 (2012) pp. 277-295

# Effect of Temperature Changes on Dynamic Pull-in Phenomenon in a Functionally Graded Capacitive Micro-beam

B. Mohammadi-Alasti[1,*], G. Rezazadeh[2], M. Abbasgholipour[3]

[1,3]*Department of Agricultural Machinery Engineering, Bonab Branch, Islamic Azad University, Bonab, Iran*
[2]*Department of Mechanical Engineering, Urmia University, Urmia, Iran*

Received 21 July 2012; accepted 26 September 2012

**ABSTRACT**

In this paper, dynamic behavior of a functionally graded cantilever micro-beam and its pull-in instability, subjected to simultaneous effects of a thermal moment and nonlinear electrostatic pressure, has been studied. It has been assumed that the top surface is made of pure metal and the bottom surface from a metal–ceramic mixture. The ceramic constituent percent of the bottom surface ranges from 0% to 100%. Along with the Volume Fractional Rule of material, an exponential function has been applied to represent the continuous gradation of the material properties through the micro-beam thickness. Attentions being paid to the ceramic constituent percent of the bottom surface, five different types of FGM micro-beams have been studied. Nonlinear integro-differential thermo-electro-mechanical equation based on Euler–Bernoulli beam theory has been derived. The governing equation in the static case has been solved using Step-by-Step Linearization Method and Finite Difference Method. Fixed points or equilibrium positions and singular points of the FGM micro-beam have been determined and shown in the state control space. In order to study stability of the fixed points, beam motion trajectories have been drawn, with different initial conditions, in the phase plane. In order to find the response of the micro-beam to a step DC voltage, the nonlinear equation of motion has been solved using Galerkin-based reduced-order model and time histories and phase portrait for different applied voltages and various primal temperatures have been illustrated. The effects of temperature change and electrostatic pressure on the deflection and stability of FGM micro-beams having various amounts of the ceramic constituent have been studied .



**Keywords:** MEMS; FGM; Cantilever micro-beam; Thermal; Electrical; Dynamic pull-in voltage; Instability

## 1 INTRODUCTION

IN material sciences, a functionally graded material (FGM) is a type of material whose composition is designed to change continuously within the solid. The concept is to make a composite material by varying the micro-structure from one material to another with a specific gradient. This enables the material to have good specifications of both materials. If it is for thermal or corrosive resistance or malleability and toughness, both strengths of the material may be used to avoid corrosion, fatigue, fracture, and stress corrosion cracking [1].

The aircraft and aerospace industry and the computer circuit industry are very interested in the possibility of materials that can withstand very high thermal gradients. This is normally achieved by using a ceramic layer

* Corresponding author.
*E-mail address*: behzad.alasti@gmail.com (B. Mohammadi-Alasti).

connected with a metallic layer. The concept of FGM was first considered in Japan in 1984 during a space plane project. The FGM materials can be designed for specific applications. For example, thermal barrier coatings for turbine blades (electricity production), armor protection for military applications, fusion energy devices, biomedical materials including bone and dental implants, space/aerospace industries, automotive applications, etc [1].

Due to their increased application they have been considered widely in research efforts in many engineering fields during the last few years. So it's very important to know and analysis the static and dynamic behavior of the FGM structures. Dynamic and static analysis of FGM beams has been considered in many researches in the macroscopic scale until now [2-17]. Sankar [2] gave an elasticity solution based on the Euler– Bernoulli beam theory for functionally graded beam subjected to static transverse loads by assuming that Young's modulus of the beam vary exponentially through the thickness. Zheng Zhong and Tao Yu [3] presented a general solution of a cantilever functionally graded beam with arbitrary graded variations of material property distribution based on 2D theory of elasticity. Chakraborty et al. [4] proposed a new beam finite element based on the first-order shear deformation theory to study the thermo-elastic behavior of functionally graded beam structures. In [4], static, free and wave propagation analysis are carried out to examine the behavioral difference of functionally graded material beam with pure metal or pure ceramic. Chakraborty and Gopalakrishnan [5] analyzed the wave propagation behavior of FG beam under high frequency impulse loading, which can be thermal or mechanical, by using the spectral finite element method. Kapuria et al. [6] validated a third order zigzag theory based model for layered functionally graded beams in conjunction with the modified rule of mixtures (MROM) for effective modulus of elasticity through experiments for static and free vibration response. Aydogdu and Taskin [7] investigated the free vibration behavior of a simply-supported FG beam by using Euler–Bernoulli beam theory, parabolic shear deformation theory and exponential shear deformation theory. Gharib et al. [8] worked on smart structures and presented an analytical solution of functionally graded beams with piezoelectric sensory and actuator layers**.** Piovan and Sampaio [9] studied on the vibrations of flexible sliding functionally graded material beams and derived a formulation for these beams based on Euler-Bernoulli theory. Because thermal environment induced dynamic behavior in FGM materials so Xiang and Shi [10] studied static analysis of functionally graded piezoelectric (FGMPM) actuators or sensors under one-dimensional heat conduction. Ying et al. [11] obtained the exact solutions for bending and free vibration of FG beams resting on a Winkler–Pasternak elastic foundation based on the two dimensional elasticity theory by assuming that the beam is orthotropic at any point and the material properties vary exponentially along the thickness direction. Sina et al. [12] used a new beam theory different from the traditional first-order shear deformation beam theory to analyze the free vibration of FG beams. Simsek and Kocatürk [13, 14] investigated the free and forced vibration of a functionally graded beam subjected to a concentrated moving harmonic load and solved the governed dynamic equation of motion by using the implicit time integration Newmark- $\beta$ method. Also Simsek [15] analyzed fundamental frequency of functionally graded (FG) beams having different boundary conditions within the framework of the classical, the first-order and different higher-order shear deformation beam theories. Khalili et al. [16] presented a mixed method to study the dynamic behavior of functionally graded (FG) beams subjected to moving loads. The theoretical formulations are based on Euler–Bernoulli beam theory, and the governing equations of motion of the system are derived using the Lagrange equations. Mahi et al. [17] presented exact solutions to study the free vibration of a beam made of symmetric functionally graded materials. The formulation used is based on a unified higher order shear deformation theory. The beam is assumed to be initially stressed by a temperature rise through the thickness. All these reviewed papers are in macroscopic scales.

Recently, FGMs are widely used in micro- and nano-structures such as thin films in the form of shape memory alloys [18, 19], micro- and nano-electromechanical systems (MEMS and NEMS) [20–22] and also atomic force microscopes (AFMs) [23].

MEMS devices are generally classified according to their actuation mechanisms. One of the most important actuation mechanisms is electrostatic [24]. Study of micro-electromechanical systems, micro-sensors and micro-actuators driven by an electrostatic force are very important because of their small size, batch production, low energy consumption, low cost and compatibility with the integrated circuits (ICs). These systems are main components of many devices such as switches [25], micro-mirrors [26], micro-resonators [27], micro-actuators [28], accelerometers [29], and tunable capacitors [30].

Micro-beams under voltage driving are widely used in many MEMS devices such as capacitive micro-switches and resonant micro-sensors. These devices are fabricated, to some extent, in a more mature stage than some other MEMS devices. As the micro-structure is balanced between electrostatic attractive force and mechanical (elastic) restoring force, both electrostatic and elastic restoring forces are increased when the electrostatic voltage increases. When the voltage reaches the critical value, pull-in instability happens. Pull-in is at the point which the elastic restoring force can no longer balance the electrostatic force. Further increasing the voltage will cause the structure to

have dramatic displacement jump which causes structure collapse and failure. Pull-in instability is a snap-through like behavior and it is saddle-node bifurcation type of instability [31]. In micro-mirrors [26] and micro-resonators [27] ,the designer avoids this instability to achieve stable motions, while in switching applications [32] the designer exploits this effect to optimize device's performance. Hence, it is important to pay attention to static and dynamic behavior of the ceramic-metallic FGM micro-beams.

Since it is sometimes difficult for a single layer to meet all material and economical requirements posed to an MEMS structural layer, Witvrouw and Mehta [21] proposed the use of a non-homogenous functionally graded material (FGM) layer to achieve the desired electrical and mechanical properties and suggested that a polycrystalline-SiGe (poly-SiGe) layer can be an appropriate choice. Hasanyan et al. [33] studied the pull-in instabilities in a functionally graded MEMS due to the heat produced by the electric current. The material properties of the two-phase MEMS are assumed to vary continuously in the thickness direction. Recently, Jia et al. [34] investigated the nonlinear pull-in characteristics of the microswitches made of either homogeneous material or non-homogeneous functionally graded material (FGM) with two material phases under the combined electrostatic and intermolecular force. The effects of material composition, gap ratio, slenderness ratio, intermolecular force, axial residual stress on the pull-in instability were shown.

Temperature change is one of the basic actuation parameters that can tune the system directly. Thermal actuation is known for its capability in producing a large and linear displacement with respect to a heating power. This mechanism is derived using a FGM micro-beam including variable thermal expansion coefficient along its thickness. In some applications of micro-beams such as micro-capacitive thermal sensors and thermal tunable capacitors, the used micro-beam is not only subjected to an electrostatic force but also to a thermal bending moment. In addition, all of the micro-actuators and micro-sensors are exposed to temperature changes due the energy loss of the devices or changes of the environmental temperature. Temperature changes by creating a thermal moment significantly affect the mechanical behavior and pull-in parameters of electro-statically actuated micro devices, but there are not enough studies on the effect of temperature changes on the stability of micro-beams especially FGM micro-beams. Therefore ,the objective of the present investigation is to study the static and dynamic response of a FGM cantilever micro-beam and its instability (pull-in phenomenon), when it is actuated simultaneously by nonlinear electrostatic forces and thermal bending moments. The critical values of the voltage in the presence of the temperature changes, which lead the structure to an unstable condition by undergoing to a saddle node bifurcation in the case of statically application of voltage and through a homo clinic bifurcation in the case of a step DC voltage application, are determined.

## 2 MODEL DESCRIPTION AND MATHEMATICAL MODELING

The suggested model includes a deformable FGM cantilever micro-beam separated from a fixed ground plate as a substrate by an air gap $g_0$ ( Fig. 1).

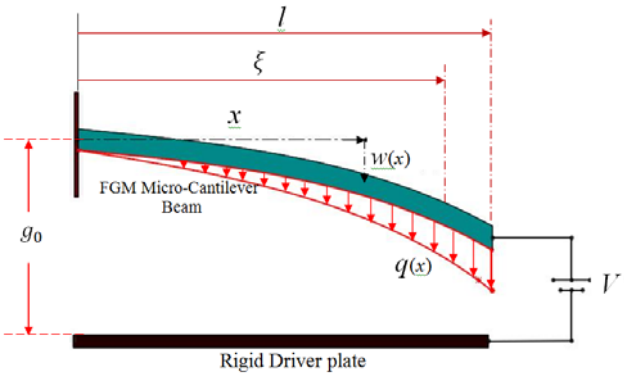


**Fig. 1**
Schematic view of a FGM cantilever micro-beam after deformation.

Between the capacitor electrodes (deformable FGM cantilever micro-beam and ground plate), a DC voltage source, *V,* is used to create an electrostatic force along the micro-beam.

The following factors can cause a deflection in the micro-beam:

- Temperature changes (varying thermal expansion coefficient of FGM micro-beam along its thickness cause the deflection of the micro-beam as a result of temperature changes).
- Electrostatic force resulting from an applied voltage.

In the present work, mechanical behavior of the micro-beam is studied considering two loading cases:

- Applying a DC voltage statically and changing the temperature in system.
- Applying a step DC voltage to the thermally deflected micro-beam.

Fig. 2 shows a part of FGM cantilever micro-beam schematically. Assume a micro-beam with length $l$, thickness $h$, width $b$, cross sectional area $A$, thermal expansion coefficient $\alpha$, material density $\rho$ and Young's modulus $E$, which are varying along the beam thickness. $w$ is the deflection of the micro-beam. Let $x$ be the coordinate along the micro-beam with its origin at the left end, and $z$ be the coordinate along the cross section with its origin at the mid plane of the micro-beam. Parameter $\tilde{z}$ denotes the distance of an assumed point from the top surface.

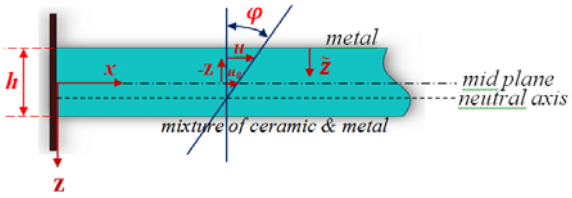


**Fig. 2**
A part of the FGM cantilever micro-beam: a) side view; b) section view.

The micro-beam is subject to a viscous damping, which is approximated by an equivalent damping coefficient $c$ per unit length.

In view of the fact that FGMs are typically made from a mixture of metal and ceramic, their material properties are related to both the metal and ceramic properties and the continual distribution of the constituent materials.

It is assumed that the material properties of FGM micro-beam vary along its thickness [15, 35-37], and the top surface is made of pure metal but the bottom surface from a mixture of metal and ceramic. Subscript "c" for ceramic and "m" for metal is used.

Noda and Jin [36] considered exponential functions for representation of continuous gradation of the material properties in analytical solution of FGM problems:

$$E = E_m e^{\gamma \tilde{z}},\ \alpha = \alpha_m e^{\beta \tilde{z}},\ \rho = \rho_m e^{\delta \tilde{z}} \tag{1}$$

$\gamma$, $\beta$ and $\delta$ are constants where their values depend on the dispersion of the ceramic into the metal.

The exponential rules usually make the problem easier to solve and can actually provide a much better approximation than some other rules, e.g., linear functions, especially for the mechanical properties [37].

There are four important points on this problem. First, to have a large and sensible deflection, the expansion coefficients of metal and ceramic should be with high different values. Second, the bottom surface of the micro-beam should be conductive as an electrode for creating electrostatic pressure, thus bottom surface of the beam can be covered with a golden thin layer at nano thickness. Third, because of micro scales, the corresponding Biot number of the problem is about $10^{-8}$ and it is suitable -with good accuracy- to take uniform temperature distribution in the beam. Fourth, pay attention to sizes and materials used for model, ratio of thickness to length scale parameter is about 40, that for ratio more than 10, the results predicted by the classical beam theory are approximately equal to those developed by the modified couple stress theory [38].

### *2.1 Non-linear static equation dominant in FGM cantilever micro-beam*

As a result of temperature variation in the system, the mid plane of the FGM micro-beam is stretched. $u_0$ is the displacement or extension of the mid plane in $x$ direction and $u$ is the total extension along $x$-axis of a layer located at a given distance $z$ Fig. 2.

For selected micro-beam, $h/l$ ratio is usually small enough to neglect the shear deformation. Total strain at x direction at a given cross section of the micro-beam based on Euler–Bernoulli beam theory can be written as follows in terms of longitudinal displacement [39]:

$$\varepsilon_x = \frac{du}{dx},\ \left(u = u_0 - z\frac{dw}{dx}\right) \tag{2}$$

Using Hook's law and Eq. (2), the relationship between the stress, strain and temperature changes for Euler–Bernoulli beam in a cross section area of the micro-beam can be expressed as [40]:

$$\sigma_x = E\left(\varepsilon_x - \alpha\theta\right) = E\left(\frac{du_0}{dx} - z\frac{d^2w}{dx^2}\right) - E\alpha\theta \tag{3}$$

where $\theta$ is temperature change, measured with respect to an initial temperature $T_0$. Of course, it is considered that there exist a plane stress condition and for a wide beam (for the plane strain condition) $E$ must be replaced by $E/\left(1-\nu^2\right)$ and $\alpha$ by $\alpha/\left(1-\nu\right)$. The equation of FGM cantilever micro-beam static deflection can be obtained as [40]:

$$-\left(EI\right)_{eq}\frac{d^2w}{dx^2} = M\left(x\right) + M^T \tag{4}$$

where

$$\left(EI\right)_{eq} = \frac{bE_m\left[2\cosh\left(\gamma h\right) - \left(\gamma h\right)^2 - 2\right]}{\gamma^3\left(1-e^{-\gamma h}\right)} \tag{5}$$

$$M^T = \Omega\theta,\ \ \Omega = \left[\frac{bE_m\alpha_m}{\gamma\left(1-e^{-\gamma h}\right)\left(\gamma+\beta\right)^2}\left[\gamma h\left(\gamma+\beta\right)\left(1-e^{\beta h}\right) + \beta\left(e^{\gamma h}-1\right)\left(e^{\beta h}-e^{-\gamma h}\right)\right]\right] \tag{6}$$

$M^T$ is the thermal moment and $M(x)$ is the external bending moment in a given section resulting from the electrostatic pressure acting along the micro-beam. With respect to Fig. 1, $M(x)$ can be expressed as [25]:

$$M\left(x\right) = -\int_x^l q\left(\xi\right)\left(\xi - x\right)d\xi,\ \ q\left(\xi\right) = \frac{\varepsilon_0 bV^2}{2(g_0 - w(\xi))^2} \tag{7}$$

where $q(\xi)$ is the electrostatic force per unit length of the micro-beam, $\varepsilon_0$ and $V$ are the permittivity of air and the voltage applied to the micro-beam and substrate, respectively.

*2.2 Differential equation dominant in dynamic behavior of FGM cantilever micro-beam*

Considering inertia term of the beam, the governing differential equation for dynamic deflection $w(x,t)$ of the FGM cantilever micro-beam can be obtained as [28, 41, 42]:

$$\left(EI\right)_{eq}\frac{\partial^4 w}{\partial x^4} + \left(\rho A\right)_{eq}\frac{\partial^2 w}{\partial t^2} + c\left(\frac{\partial w}{\partial t}\right) = \frac{\varepsilon_0 bV^2}{2\left(g_0 - w\right)^2} \tag{8}$$

where

$$\left(\rho A\right)_{eq} = \frac{b\rho_m}{\delta}\left(e^{\delta h} - 1\right) \tag{9}$$

$t$ and $c$ are time and equivalent damping coefficient per unit length of the beam, respectively. The boundary conditions $G(w)$ for the FGM cantilever micro-beam are [28, 41, 42]:

$$\mathrm{G(w)}: \begin{cases} w(x,t)\big|_{x=0} = 0, \ \dfrac{\partial w(x,t)}{\partial x}\bigg|_{x=0} = 0 \\ \dfrac{\partial^2 w(x,t)}{\partial x^2}\bigg|_{x=l} = -\dfrac{M^T}{\left(EI\right)_{eq}}, \ \dfrac{\partial^3 w(x,t)}{\partial x^3}\bigg|_{x=l} = 0 \end{cases} \tag{10}$$

## 3 NUMERICAL SOLUTION

### *3.1 Temperature changes in the cantilever micro-beam (no applied voltage)*

When the applied voltage is zero, there is no Electrostatic Pressure and the external bending moment at a cross section is zero. Therefore,the equation of FGM micro-beam deflection at a given $x$, along its length can be obtained as below in terms of temperature changes [40]:

$$\mathrm{w_{OT}} = -\frac{\Omega\theta}{2\left(\mathrm{EI}\right)_{\mathrm{eq}}}\mathrm{x}^2 \tag{11}$$

### *3.2 Temperature changes in the electro-statically deflected micro-beam*

Solution of nonlinear integro-differential Eq. (4), due to its nonlinear nature, is more complex and time consuming. In order to overcome the complexity, it is common to linearize it. Since the deflection of the micro-beam $\left(\mathrm{w}\right)$ is high enough as compared to the gap $\left(\mathrm{g_0 - w}\right)$, the linearization of Eq. (4) with respect to the initial position causes considerable errors in the results. Therefore, stepwise applying of voltage and temperature as a method called Step-by-Step Linearization Method (SSLM) is proposed [28]. In this method the nonlinear equation is linearized in each step with respect to the previous one. At last, a linear equation in terms of the difference of the micro-beam deflection between two successive steps $\left(\psi(\mathrm{x})\right)$ is derived and solved using Finite Difference Method (FDM). By selecting small step sizes for the applied voltage and temperature changes, $\psi(\mathrm{x})$ is small enough and $w\left(x\right)$ can be calculated with acceptable accuracy.

Assume $T_i$ and $V_i$ to be the temperature and the applied voltage in ith step, which cause a deflection $w_i\left(x\right)$ in the micro-beam. Increasing the temperature and the applied voltage in the (i+1)th step causes a growth $\left(\psi(\mathrm{x})\right)$ in the micro-beam deflection as follows [40]:

$$\begin{aligned} &T_{i+1} = T_i + \delta T \ \ \& \ \ V_{i+1} = V_i + \delta V \\ &\Rightarrow \ w_{i+1} = w_i + \delta w = w_i + \psi\left(x\right), \ \ i = 1,2,\ldots,N \end{aligned} \tag{12}$$

where $\delta T$ and $\delta V$ are the temperature and the voltage growth between two successive steps, respectively.

Considering that $w_i\left(x\right)$ and $w_{i+1}\left(x\right)$ satisfy the differential equation of the micro-beam deflection, the linear equation for $\psi\left(x\right)$ can be expressed as [40]:

$$(EI)_{eq}\frac{d^2\psi(x)}{dx^2}-\psi(x)\int_x^l\frac{\varepsilon_0 bV_i^2}{\left(g_0-w_i(\xi)\right)^3}(\xi-x)d\xi=\int_x^l\frac{\varepsilon_0 bV_i\delta V}{\left(g_0-w_i(\xi)\right)^2}(\xi-x)d\xi-\delta M^T \tag{13}$$

For a cantilever micro-beam, the corresponding boundary conditions are zero displacement and zero slope in the fixed end of the micro-beam. The unknown function $\psi(x)$ also satisfies the same boundary conditions.

Now that nonlinear Eq. (4) has been converted to linear form Eq. (13) in terms of $\psi(x)$, using any discretizing method such as the finite difference method (FDM) and imposing appropriate boundary conditions, Eq. (13) can be solved.

*3.3 Application of a step DC voltage on the thermally deflected micro-beam*

In this case, the total deflection of the micro-beam, caused by an applied step DC voltage and a temperature rise ( $\theta$ ) can be written as:

$$w(x,t)=w_{OT}(x)+w_d(x,t) \tag{14}$$

$w_{0T}(x)$ is the static deflection of the beam owing to a temperature rise ( $\theta$ ) and $w_d(x,t)$ is the dynamic deflection owing to the applied step DC voltage ($V$). Substituting Eq. (14) into Eq. (8):

$$(EI)_{eq}\frac{\partial^4 w_{OT}}{\partial x^4}+(EI)_{eq}\frac{\partial^4 w_d}{\partial x^4}+(\rho A)_{eq}\frac{\partial^2 w_d}{\partial t^2}+c\left(\frac{\partial w_d}{\partial t}\right)=\frac{\varepsilon_0 bV^2}{2(g_0-w_{OT}-w_d)^2} \tag{15}$$

According to Eq. (11), first term of Eq. (15) is zero $\left((EI)_{eq}\frac{\partial^4 w_{OT}}{\partial x^4}=0\right)$, and also according to Eqs. (10) and (11), the boundary conditions of dynamic deflection are:

$$w_d\big|_{x=0}=0,\ \left.\frac{\partial w_d}{\partial x}\right|_{x=0}=0,\ \left.\frac{\partial^2 w_d}{\partial x^2}\right|_{x=l}=0,\ \left.\frac{\partial^3 w_d}{\partial x^3}\right|_{x=l}=0 \tag{16}$$

For convenience, the following non-dimensional variables are used:

$$\tilde{w}_{OT}=\frac{w_{OT}}{g_0},\ \tilde{w}_d=\frac{w_d}{g_0},\ \tilde{x}=\frac{x}{l},\ \tilde{t}=\frac{t}{t^*},\ t^*=\sqrt{\frac{(\rho A)_{eq}\,l^4}{(EI)_{eq}}} \tag{17}$$

As a result ,Eq. (29) can be written as follows:

$$\frac{\partial^4\tilde{w}_d}{\partial\tilde{x}^4}+\frac{\partial^2\tilde{w}_d}{\partial\tilde{t}^2}+\tilde{c}\left(\frac{\partial\tilde{w}_d}{\partial\tilde{t}}\right)=\frac{\tilde{V}^2}{\left(1-\tilde{w}_{OT}-\tilde{w}_d\right)^2} \tag{18}$$

where

$$\tilde{c}=\sqrt{\frac{cl^2}{(EI)_{eq}(\rho A)_{eq}}},\ \tilde{V}^2=\frac{\varepsilon_0 bV^2l^4}{2(EI)_{eq}\,g_0^3} \tag{19}$$

Different methods are available for solving the linear and non-linear differential equations. Among them, weighted residuals approach is considered. In this method, for solving a dynamic equation, firstly the shape functions must be considered, and then, along with Galerkin-Bubnov procedure, must be applied. An approximate N-term solution for deriving small vibrations of the micro-beam is defined as:

$$\tilde{w}_d\left(\tilde{x},\tilde{t}\right)=\sum_{n=1}^{N}\varphi_n\left(\tilde{x}\right)T_n\left(\tilde{t}\right) \tag{20}$$

where, $T_n\left(\tilde{t}\right)$ and $\varphi_n\left(\tilde{x}\right)$ are functions of time and shape, respectively. The shape function must satisfy the geometrical boundary conditions. Therefore, by substituting the approximate solution into the vibration Eq. (18), the following error function will be obtained:

$$\sum_{n=1}^{N}\varphi_n^4\left(\tilde{x}\right)T_n\left(\tilde{t}\right)+\sum_{n=1}^{N}\varphi_n\left(\tilde{x}\right)\ddot{T}_n\left(\tilde{t}\right)+\tilde{c}\sum_{n=1}^{N}\varphi_n\left(\tilde{x}\right)\dot{T}_n\left(\tilde{t}\right)-\frac{\tilde{V}^2}{\left(1-\tilde{w}_{OT}-\tilde{w}_d\right)^2}=E_r(\tilde{x},\tilde{t}) \tag{21}$$

where $E_r\left(\tilde{x},\tilde{t}\right)$ is the residual value or error value. Using the weight function $\varphi_j\left(\tilde{x}\right)$ similar to the shape function and applying Galerkin-Bubnov procedure, a set of N nonlinear ordinary differential equations with respect to time can be obtained as:

$$\int_0^1\varphi_j\left(\tilde{x}\right)E_r(\tilde{x},\tilde{t})d\tilde{x}=0,\quad j=1,2,\ldots,N \tag{22}$$

By using Eq. (22), ordinary dynamics equation can be obtained as follows:

$$\sum_{n=1}^{N}M_{jn}\ddot{T}_n\left(\tilde{t}\right)+\sum_{n=1}^{N}C_{jn}\dot{T}_n\left(\tilde{t}\right)+\sum_{n=1}^{N}K_{jn}T_n\left(\tilde{t}\right)=F_j,\quad j=1,2,\ldots,N \tag{23}$$

where

$$M_{jn}=\int_0^1\varphi_j\left(\tilde{x}\right)\varphi_n\left(\tilde{x}\right)d\tilde{x}\ ,\quad C_{jn}=\tilde{c}\int_0^1\varphi_j\left(\tilde{x}\right)\varphi_n\left(\tilde{x}\right)d\tilde{x}\ ,\quad K_{jn}=\int_0^1\varphi_j\left(\tilde{x}\right)\varphi_n^4\left(\tilde{x}\right)d\tilde{x}$$
$$F_j=\int_0^1\frac{\varphi_j\left(\tilde{x}\right)\tilde{V}^2d\tilde{x}}{\left(1-\tilde{w}_{OT}-\tilde{w}_d\right)^2} \tag{24}$$

Here, $M_{jn},C_{jn},K_{jn}$ and $F_j$ are mass, damping, system stiffness, and force vectors, respectively. It must be noted that due to the nonlinear nature of electrostatic force integration of the forcing term ($F_j$) must be repeated at any time step.

## 4 NUMERICAL RESULTS AND DISCUSSION

The studied micro-beam in this paper has the material and geometrical properties shown in Tables 1. and 2. They are reference values for any case where no values are given. High difference of thermal expansion coefficients of two materials (Aluminum and Alumina) is suitable to have a large and sensible deflection.

Bin and Wanji [44] represented that Aluminum length scale parameter $\left(l_s\right)$ estimated from the experimental data is $0.15\mu m$. Thus, the ratio of thickness to length scale parameter $\left(h/l_s\right)$ for this model is about 40. And since

Asghari et al. [38] showed that for $h/l_s \rangle 10$, the results predicted by the classical beam theory are approximately equal to those developed by the modified couple stress theory, therefore for this model, the Euler–Bernoulli beam theory (classical) is acceptable with good accuracy.

**Table 1**
Geometrical properties of the FGM micro-beam [40].

| Parameters | Values |
|---|---|
| Length ($l$) | 500 $\mu m$ |
| Width ($b$) | 90 $\mu m$ |
| Thickness ($h$) | 6 $\mu m$ |
| Initial gap ($g_0$) | 2 $\mu m$ |
| Permittivity of air ($\varepsilon_0$) | 8.85 $pF/m$ |

**Table 2**
Material properties (P) of the FGM micro-beam [43].

| Parameters | Values | |
|---|---|---|
| | Metal (m) | Ceramic (c) |
| Material type | Aluminum $(Al)$ | Alumina $(AL_2O_3)$ |
| Young's modulus ($E$) | 69 $GPa$ | 390 $GPa$ |
| Thermal expansion Coefficient ($\alpha$) | $23.1\times10^{-6}\ ^\circ k^{-1}$ | $7.7\times10^{-6}\ ^\circ k^{-1}$ |
| Density ($\rho$) | 2700 $kg/m^3$ | 3960 $kg/m^3$ |

To verify the model, obtained results for some special cases were compared to those published in some references. First a FGM micro-beam having material and geometrical properties of ref. [40] is considered and observed that the obtained static pull-in voltage is in good agreement with that published in [40]. For the dynamic case ,it was reported that the dynamic pull-in voltage is about 92% of static one [45-47], and as seen the obtained value for the dynamic pull-in voltage in our model is 92% of the static one.

It is assumed that the top surface is of pure metal but the bottom surface from a mixture of metal and ceramic and that ceramic constituent percent of bottom surface ranges from 0% to 100%. In order to determine material properties of the bottom surface ($P_h$), volume fraction of material is used [48-51]:

$$P_h = P_{(\tilde{z}=h)} = V_c P_c + V_m P_m \tag{25}$$

where $V_c$ and $V_m$ are the ceramic and metal volume fractions and $P_c$ and $P_m$ are the ceramic and metal properties.

Meanwhile, exponential functions are used for representation of continuous gradation of the material properties through the micro-beam thickness (between the top and bottom surfaces) [36, 51 , 52]:

$$E_{\tilde{z}} = E_m e^{\gamma \tilde{z}},\ \ \alpha_{\tilde{z}} = \alpha_m e^{\beta \tilde{z}},\ \ \rho_{\tilde{z}} = \rho_m e^{\delta \tilde{z}} \tag{26}$$

Therefore, using Eqs. (25) and (26), the constants $\gamma, \beta$ and $\delta$ can be obtained as:

$$\gamma = \frac{1}{h} ln\left(\frac{E_h}{E_m}\right),\ \ \beta = \frac{1}{h} ln\left(\frac{\alpha_h}{\alpha_m}\right),\ \ \delta = \frac{1}{h} ln\left(\frac{\rho_h}{\rho_m}\right) \tag{27}$$

Attentions being paid to the ceramic constituent percent of the bottom surface, five different types of FGM micro-beams were considered and their characteristics are given in Table 3.

The first type is in fact a simple and homogeneous classic beam made of pure metal. For type 5, the top and bottom surfaces are from pure metal and pure ceramic, respectively. Type 5 is the reference type for any where no type is identified.

**Table 3**
Characteristics of five different types of FGM micro-beams.

| Type | Ceramic percent of bottom surface | $V_c$ | $E_h$ GPa | $\alpha_h$ $(10^{-6}/°K)$ | $\rho_h$ $(kg/m^3)$ | $\gamma$ | $\beta$ | $\delta$ |
|---|---|---|---|---|---|---|---|---|
| 1 | 0 % | 0.00 | 69.00 | 23.10 | 2700 | 0.0 | 0.0 | 0.0 |
| 2 | 25 % | 0.25 | 149.25 | 19.25 | 3015 | 128586.0 | -30386.9 | 18391.3 |
| 3 | 50 % | 0.50 | 229.50 | 15.40 | 3330 | 200299.4 | -67577.1 | 34953.4 |
| 4 | 75 % | 0.75 | 309.75 | 11.55 | 3645 | 250276.5 | -115524.5 | 50017.4 |
| 5 | 100 % | 1.00 | 390.00 | 7.70 | 3960 | 288673.3 | -183102.0 | 63832.0 |

(Status of bottom surface: Mixture of metal and ceramic); (Status of top surface: Metal rich for all types)

Diagrams of Young's modulus and thermal expansion coefficient along thickness for five types of FGM micro-beams are shown in Fig. 3.

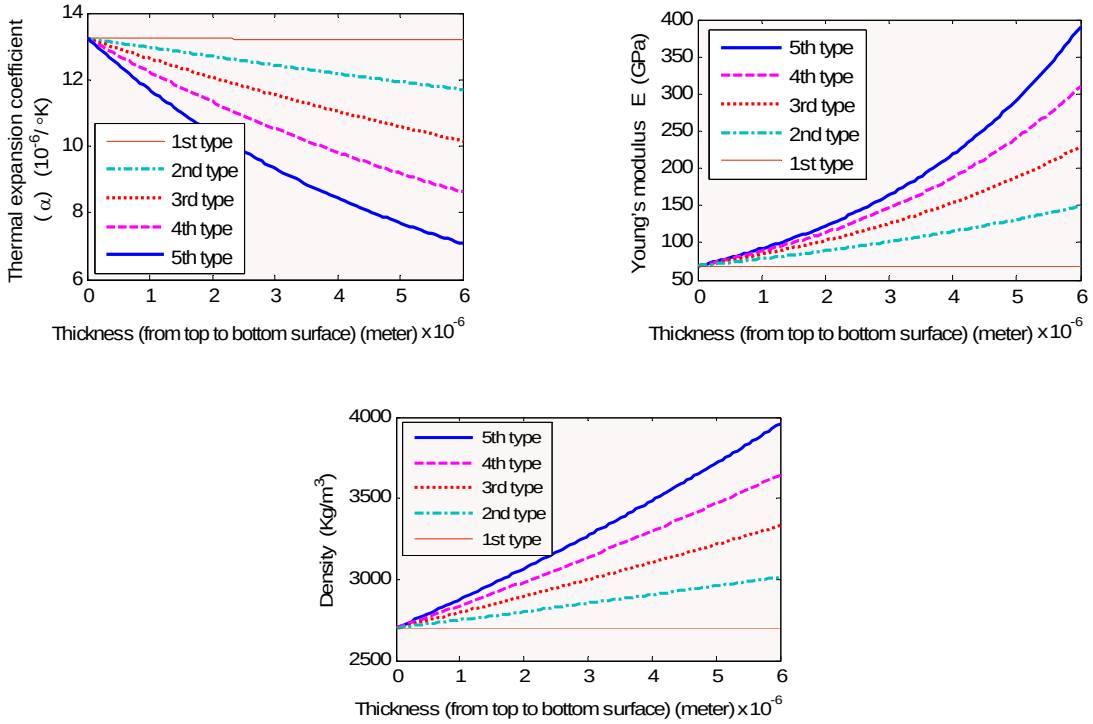


**Fig. 3**
Young's modulus, thermal expansion coefficient and density along thickness for five types of FGM micro-beams.

*4.1 Stability of equilibrium position due to statically application of DC Voltage and remperature changes*

Geometrical and physical properties of the proposed FGM model are similar to properties listed in Tables 1-3. Based on the results given in Tables 4.and 5, for type 5 FGM micro-beam, the best step size for the voltage application is 0.07 volt and the best number of the grid points is 67. The static pull-in voltage for type 5 cantilever FGM micro-beam is 11.83 volt Fig.4 , when there are no temperature changes $(\theta = 0)$.

**Table 4**
Obtained static pull-in voltages for type 5 FGM micro-beam with selection of 100 grid points and different step sizes for the applied voltage, $(\theta = 0)$.

| applied voltage step sizes $(volt)$ | 0.25 | 0.15 | 0.11 | 0.10 | 0.09 | 0.07 | 0.06 | 0.05 |
|---|---|---|---|---|---|---|---|---|
| Obtained static pull-in voltage $(volt)$ | 12.25 | 12 | 11.99 | 11.9 | 11.88 | 11.83 | 11.83 | 11.83 |

**Table 5**
Obtained static pull-in voltages for type 5 FGM micro-beam with value of $0.07(volt)$ for the voltage step size and different grid points, $(\theta = 0)$.

| Number of grid points | 100 | 80 | 70 | 67 | 65 |
|---|---|---|---|---|---|
| Obtained static pull-in voltage $(volt)$ | 11.83 | 11.83 | 11.83 | 11.83 | 11.76 |

Fig. 4 shows the equilibrium positions or fixed points of the cantilever micro-beam versus applied voltage as a control parameter. As shown in Fig. 4, for a given applied voltage the micro-beam has three fixed points or equilibrium positions. In addition to the fixed points ,of course ,the position of the substrate as a singular point plays an important role in the mechanical behavior of the micro-beam. Figs. 5a-5c show phase portrait of the micro-beam for different applied voltages and different initial conditions. Paying attention to Figs. 5a-5c, it can be found that for a given applied voltage, the first equilibrium position is a stable centre, the second is a unstable saddle node and the third is a mathematically stable centre but physically impossible due to its location underneath the substrate. As shown in Figs. 5a-5c, there are two basins of attraction of stable centers and a basin of repulsion of unstable saddle node. Depending on the location of the initial condition, the system can be stable or unstable. As shown in Figs. 5a-5c the velocity of the system near to the substrate position, due to the singularity in the electrostatic force, rapidly approaches infinity.

In addition, as shown in Fig. 4 in the state-control space, the stable and unstable branches of the fixed points, with increasing applied voltage, meet together at a saddle-node bifurcation point. The voltage corresponding to the saddle-node bifurcation point is a critical value, which is well-known as the static pull-in voltage in the MEMS literature.

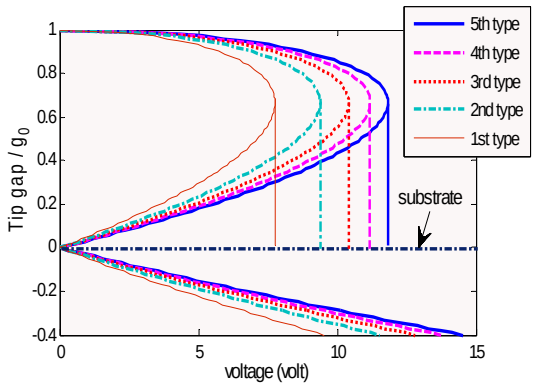


**Fig. 4**
The tip gap versus applied voltage for 5 types of FGM micro-beams, (θ=0).

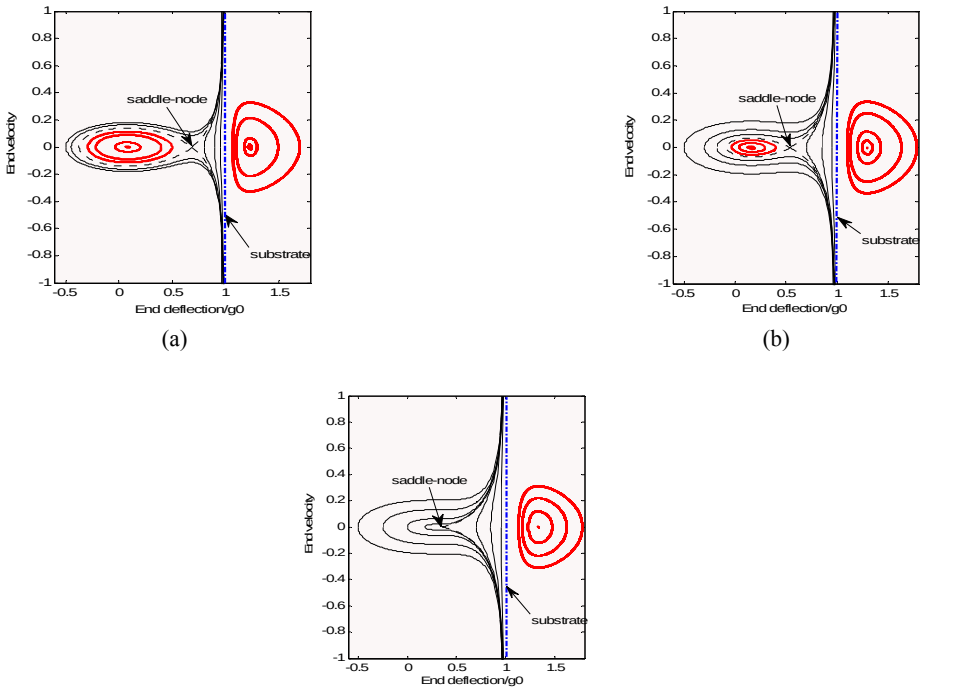


**Fig. 5**
Phase portraits of the micro-beam with different initial conditions for the FGM micro-beam (type 5) a) V=7 volt b) V=10 volt c) at the pull-in voltage when there are no viscous damping effect and no temperature changes.

Also at Fig. 5, it is clear that by increasing voltage, first attraction basin is get smaller and the stable center and the unstable saddle node are closer together. Until at static pull-in voltage, these points meet together and first attraction basin is disappeared.

In addition Fig. 4 shows the static pull-in phenomenon for different FGM types. And according to Fig. 4 it is clear that by growing the ceramic constituent percent due to increasing $(EI)_{eq}$ and the equivalent stiffness of the FGM micro-beam, the static pull-in voltage is increased.

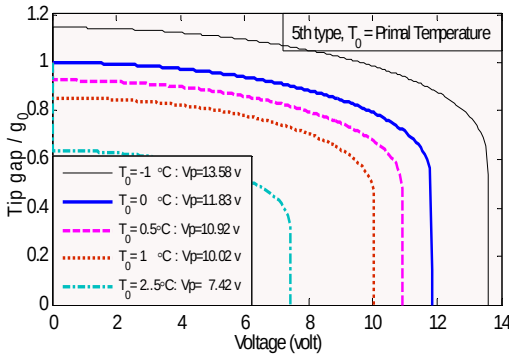


**Fig. 6**
Tip gap of the FGM micro-beam (5th type) versus applied voltage with primal temperature changes.

Fig. 6 shows the tip gap of the FGM micro-beam (5th type) versus applied voltage with different primal temperature changes. As shown ,when the micro-beam heats up the pull-in phenomenon happens earlier than when there is no temperature rise. It means that the pull-in voltage will be decreased as the primal temperature increases. For negative primal temperature changes, primal deformation of FGM micro-beam is toward up then pull-in voltage increases.

Fig. 7 shows the tip gap of the FGM micro-beam versus the temperature rise when the micro-beam deflects due to a given primal voltage and then the temperature changes increase the micro-beam deflection up to the pull-in temperature. When there is no applied voltage and micro-beam deflects by temperature changes only, there is no nonlinearity and the tip deflection varies linearly with the temperature and the system keeps its stability and it solely contacts with the ground plate. Moreover Fig. 7 shows whatever ceramic percent decreases, primal deflection due to the primal voltage increases; but there by applying temperature, for micro-beam with less ceramic, temperature effect is less and it exhibits less reflex. The classic beam (first type) due to primal voltage is deflected but temperature changes have no effect on it.

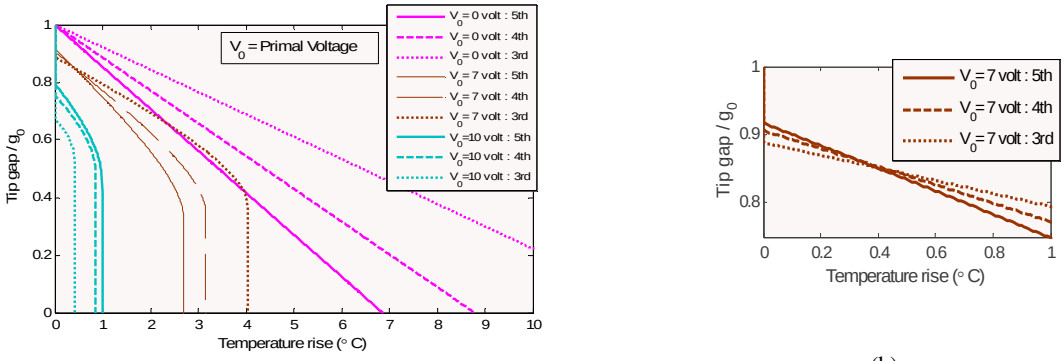


(a) (b)

**Fig. 7**
a)Tip gap versus temperature rise for 3 types of the FGM micro-beams with primal applied voltage b) zooming for $V_1$=7(*volt*).

Fig.8 illustrates the natural frequency of the micro-beam versus applied DC voltage for different types of FGM micro-beams. As shown in Fig. 8 with rising ceramic constituent percent, the value of natural frequency for a given applied voltage is increased due to growing micro-beam equivalent stiffness. In addition it is shown that the value of natural frequency is decreased by increasing the applied DC voltages until the natural frequency of the micro-beam becomes zero and static pull-in phenomenon occurs. In other word Fig. 8 emphasizes that the pull-in instability is a kind of buckling or static instability.

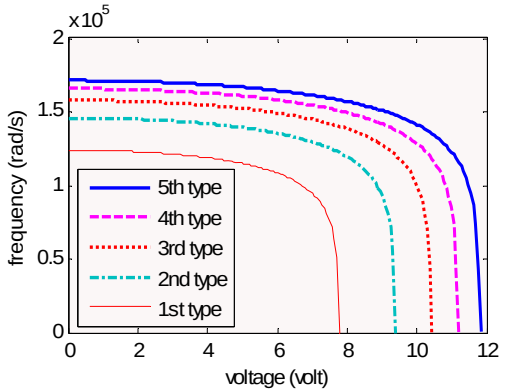


**Fig. 8**
Natural frequency of the micro-beam versus applied DC voltage for 5 types of FGM micro-beams, ( $\zeta = 0, \theta = 0$ ).

*4.2. Application of a step DC Voltage on thermally deflected micro-beam*

The step DC voltage is expressed mathematically as $V(t) = VH(t)$, where V is electrical shock amplitude and $H(t)$ is the unit step or Heaviside step function. Geometrical and physical properties of the proposed FGM model are similar to the properties listed in Tables 1-3. Before getting results, it is necessary to find the best step size for the non dimension time and the number of grid points for FDM and best number of shape functions for approximating

dynamic response. The convergence of the results for the FGM micro-beam of 5th type is listed in Tables 6-8. Based on the results given in these Tables, the best step size for the non dimension time is 0.006 and the best number of the grid points is 22 and also the best number of shape functions is 3. The dynamic pull-in voltage for the cantilever FGM micro-beam of 5th type is 10.85 volt, when there are no temperature changes and no viscous damping effect $(\theta = 0, \zeta = 0)$.

**Table 6**
Obtained pull-in voltages for FGM micro-beam of 5th type with selection of 101 grid points and different step sizes for non dimension time, $(\theta = 0, \zeta = 0)$.

| Different step sizes for non dimension time | 0.003 | 0.004 | 0.005 | 0.006 | 0.007 | 0.01 | 0.02 |
|---|---|---|---|---|---|---|---|
| Obtained dynamic pull-in voltage *(volt)* | 10.85 | 10.85 | 10.85 | 10.85 | 10.86 | 10.86 | 10.89 |

**Table 7**
Obtained dynamic pull-in voltages for FGM micro-beam of 5th type with value of 0.006 for the non dimension time step size and different grid points, $(\theta = 0, \zeta = 0)$.

| Number of grid points | 101 | 70 | 50 | 30 | 22 | 20 | 10 |
|---|---|---|---|---|---|---|---|
| Obtained dynamic pull-in voltage *(volt)* | 10.85 | 10.85 | 10.85 | 10.85 | 10.85 | 10.86 | 10.89 |

**Table8**
Obtained dynamic pull-in voltages for FGM micro-beam of 5th type with value of 0.006 for the non dimension time step size and with selection of 22 grid points and different number of shape functions, $(\theta = 0, \zeta = 0)$.

| Number of Shape Functions | 1 | 2 | 3 | 4 | 5 |
|---|---|---|---|---|---|
| Obtained dynamic pull-in voltage *(volt)* | 10.86 | 10.86 | 10.85 | 10.85 | 10.85 |

Due to dependence of the electrostatic force on both voltage and deflection (w), pull-in occurs in a voltage less than the static pull-in voltage when the voltage is applied in the form of a step DC voltage. The results of the published previous reports show that the dynamic pull-in voltage is less than about %92 static one [45-47, 53].

It must be noted that the scenario of instability in the case of applying step DC voltages is different from its statically application. As Figs. 4 and 5 showed, when the applied DC voltage approaches static pull-in voltage, the system tends to an unstable equilibrium position by undergoing to saddle node bifurcation.

A saddle node bifurcation is a locally stationary bifurcation. This kind of bifurcation can be analyzed based on locally defined eigen-values. In addition to local bifurcations, periodic orbits encounter phenomena that cannot be analyzed based on locally defined eigen-values. Such phenomena are called global bifurcations [54, 55].

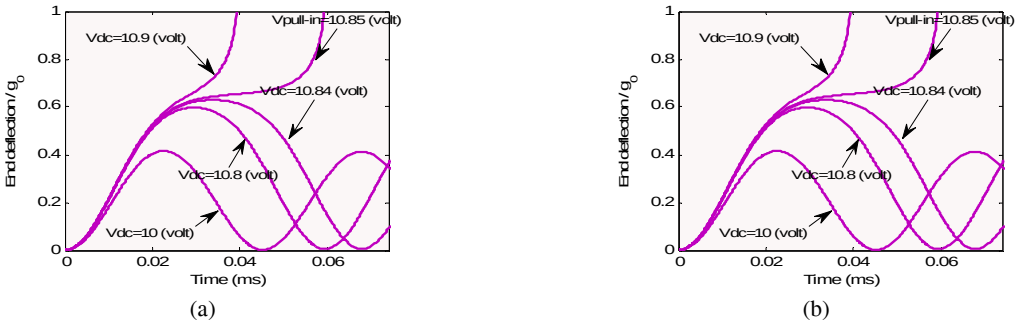


(a) (b)

**Fig. 9**
a) The time history of the normalized end deflection for the FGM micro-beam (5th type) b) phase portrait of the response, $(\theta = 0, \zeta = 0)$.

Figs. 9a and 9b show time history and phase portrait of the micro-beam response to step DC voltage. This figure shows a metamorphosis of how a periodic orbit approaches homoclinic orbit at dynamic pull-in voltage. Indeed the

periodic orbit is ended at dynamic pull-in voltage where a homoclinic orbit is formed. In another word when the applied voltage approaches dynamic pull-in voltage due to the displacement dependency of the nonlinear electrostatic force and decreasing the equivalent stiffness, period of the oscillations tends to infinity and a symmetry breaking is occurred in motion trajectories. It can be said that there happens a homoclinic bifurcation when the periodic orbit collides with a saddle point at dynamic pull-in voltage.

Fig. 10 shows the time response and phase portrait for different types of the FGM micro-beams at dynamic pull-in voltage when there are no temperature changes and viscous damping effect. By growing the ceramic percent, similar to the static pull-in voltage due to growth of equivalent stiffness of the FGM micro-beam, the dynamic pull-in voltage is increased; but due to increasing the value of pull-in voltage, the pull-in response time is decreased.

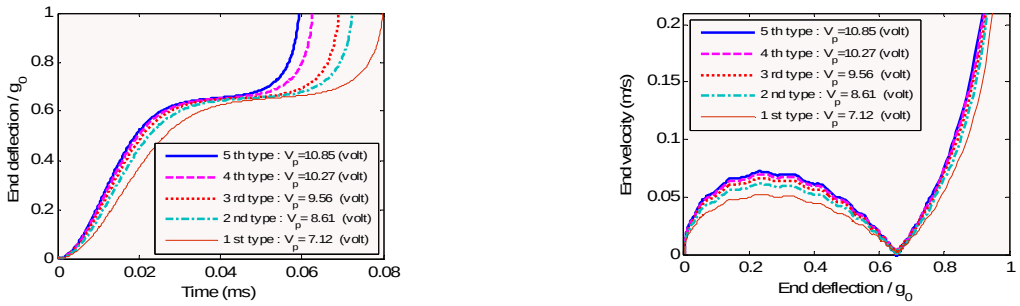


(a) (b)

**Fig. 10**
a)The time history of the normalized end deflection for different types of the FGM micro-beams at dynamic pull-in voltage b) phase portrait of the response, $(\theta = 0, \zeta = 0)$.

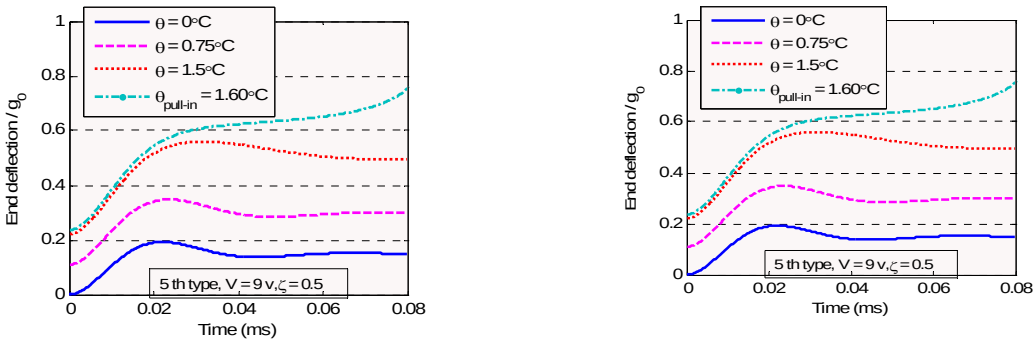


(a) (b)

**Fig. 11**
a) The time history of the normalized end deflection for the FGM micro-beam (5th type) at different primal temperatures b) phase portrait of the response, $(V = 9volt, \zeta = 0.5)$.

Fig. 11a and 11b show the time response and phase portrait of the FGM micro-beam (5th type) subjected to a temperature rise $\theta$ and a step DC voltage V. Due to viscous damping effect in the system, it returns to its static equilibrium position. As shown, temperature rise cause the larger deflection but smaller velocity.

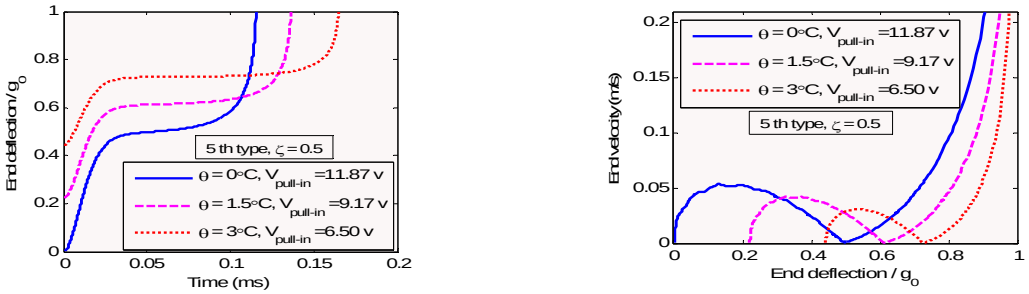


(a) (b)

**Fig. 12**
a)The time history of the normalized end deflection for the FGM micro-beam (5th type) at different primal temperatures b) phase portrait of the response, (at dynamic pull-in voltage, $\zeta = 0.5$ ).

In Fig. 12a and 12b, the step DC voltage is set to pull-in voltage, in which as increasing the temperature, the pull-in time increases due to decreasing the pull-in voltage.

Fig. 13 shows the time response and phase portrait for different types of the FGM micro-beams at dynamic pull-in voltage when the system is subjected to primal temperature change and viscous damping effect. By decreasing ceramic constituent percent, due to decreasing thermal expansion coefficient difference through layers of FGM micro-beam, primal deflection due to primal temperature change is decreased, and also by decreasing ceramic, equivalent stiffness of the micro-beam is decreased. Therefore for a given primal temperature change, by decreasing ceramic, firstly the dynamic pull-in voltage due to effect of decreasing primal thermal deflection, is increased, and next due to effect of decreasing the micro-beam stiffness, it is decreased.

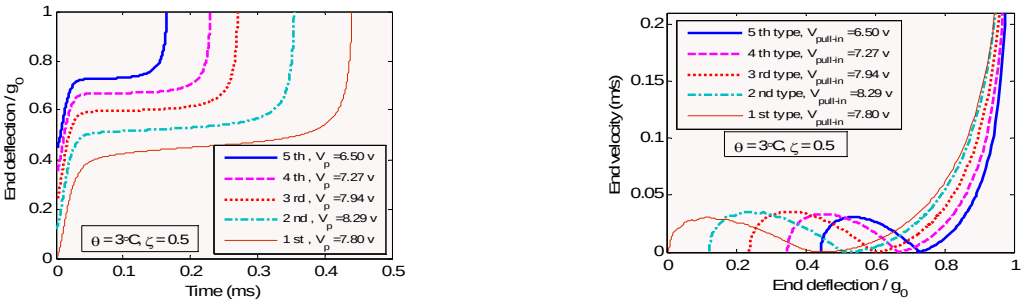


(a) (b)

**Fig. 13**
a) The time history of the normalized end deflection for different types of the FGM micro-beams at dynamic pull-in voltage b) phase portrait of the response, $\left(\theta = 3^{\circ C}, \zeta = 0.5\right)$.

**Table 9**
Dynamic pull-in voltage for different types of FGM micro-beams with different primal temperatures $\left(\zeta = 0 \quad or \quad = 0.5\right)$.

| Dynamic pull-in voltage (*volt*) | | Type of FGM micro-beam | | | | |
|---|---|---|---|---|---|---|
| | | 5*th* type | 4*th* type | 3*rd* type | 2*nd* type | 1*st* type |
| $\zeta = 0$ | $\theta = 0^{\circ C}$ | 10.85 | 10.27 | 9.56 | 8.61 | 7.12 |
| | $\theta = 1.5^{\circ C}$ | 8.38 | 8.44 | 8.39 | 8.08 | 7.12 |
| | $\theta = 3^{\circ C}$ | 5.94 | 6.62 | 7.23 | 7.55 | 7.12 |
| $\zeta = 0.5$ | $\theta = 0^{\circ C}$ | 11.87 | 11.25 | 10.49 | 9.46 | 7.8 |
| | $\theta = 1.5^{\circ C}$ | 9.17 | 9.25 | 9.21 | 8.87 | 7.8 |
| | $\theta = 3^{\circ C}$ | 6.50 | 7.27 | 7.94 | 8.29 | 7.8 |

The results of the dynamic pull-in voltage for different ceramic constituent percents and different primal temperatures are listed perfectly in Table 9. Moreover temperature changes have no effect on first type, but by increasing viscous damping coefficient, pull-in voltage is increased.

Fig. 14 shows variations of the dynamic pull-in voltage versus temperature changes for different types of FGM micro-beams ( $\zeta = 0.5$ ). The listed results in Table 9. are drawn at Fig. 14.

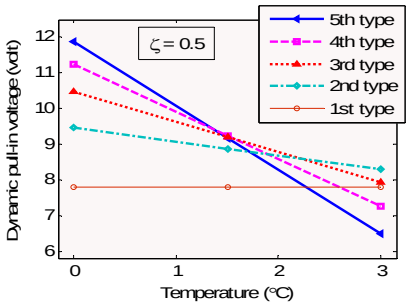


**Fig.14**
Dynamic pull-in voltage versus temperature changes for different types of FGM micro-beams ( $\zeta = 0.5$ ).

## 5 CONCLUSIONS

In this paper, a cantilever FGM micro-beam subjected to nonlinear electrostatic pressures and temperature changes was studied. It was assumed that the top surface was made of pure metal but the bottom surface from a mixture of metal and ceramic. The ceramic constituent percent of the bottom surface ranges from 0% to 100%. Considering an exponential function for representation of continuous gradation of the material properties through the micro-beam thickness, nonlinear integro-differential thermo-electro mechanical equation based on Euler–Bernoulli beam theory was derived. For static analysis, due to gradual loading, the equation was linearized using Step-by-Step Linearization Method (SSLM) and solved applying Finite Difference Method. Dynamic analysis was studied using a Galerkin-based reduced-order model. Attentions being paid to the ceramic constituent percent of the bottom surface, five different types of FGM micro-beams were studied.

It was shown that for a given applied voltage, three equilibrium positions or fixed points and a singular point exist. Based on illustrated trajectories in phase portraits, the first of them is a stable center, the second is an unstable saddle node and the third is a mathematically stable center but physically impossible because of its location (underneath the substrate). Increasing the applied voltage, as a control parameter, position of the first and second fixed points in the state-control space is closed together and at a voltage, called static pull-in voltage in MEMS literature, they meet at a saddle node bifurcation point. Results showed that by increasing percent of the ceramic constituent, the position of the saddle node bifurcation point, because of increasing the micro-beam equivalent stiffness, moves to the right in the state-control space, in other words, by increasing the ceramic constituent, the static pull-in phenomenon occurs at higher voltages.

In the case of application of a step DC voltage it was shown that periodic orbits are ended at the dynamic pull-in voltage and a homoclinic orbit is formed, it means that the structure undergoes to an unstable condition through a global homoclinic bifurcation. According to the obtained results for application of a step DC voltage on thermally actuated micro-beam, when the temperature changes get higher, the pull-in voltage decreases and consequently the pull-in time increases. For a given primal temperature change, by decreasing the ceramic constituent percent, firstly the dynamic pull-in voltage due to decreasing the primal thermal deflection, was increased and next due to decreasing the micro-beam stiffness, it was decreased. Also the effect of viscous damping on the pull-in phenomenon was shown. Obtained results can be useful for the MEMS community and those works on FGM micro-beams.

## ACKNOWLEDGEMENTS

The authors were supported by grants from the Research Office of Islamic Azad University, Bonab branch.

## REFERENCES


[1] Simsek M., 2010, Vibration analysis of a functionally graded beam under a moving mass by using different beam theories, *Composite Structures* **92**: 904–917.

[2] Sankar B.V., 2001, An elasticity solution for functionally graded beams, *Composite Science and Technology* **61**(5): 689–696.

[3] Zhong Z., Yu T., 2007, Analytical solution of a cantilever functionally graded beam, *Composites Science and Technology* **67**: 481-488.

[4] Chakraborty A., Gopalakrishnan S., Reddy J.N., 2003, A new beam finite element for the analysis of functionally graded materials, *International Journal of Mechanic Science* **45**(3): 519–539.

[5] Chakraborty A., Gopalakrishnan S., 2003, A spectrally formulated finite element for wave propagation analysis in functionally graded beams, *International Journal of Solids and Structures* **40**(10): 2421–2448.

[6] Kapuria S., Bhattacharyya M., Kumar A.N., 2008, Bending and free vibration response of layered functionally graded beams: A theoretical model and its experimental validation, *Composite Structures* **82**(3): 390-402.

[7] Aydogdu M., Taskin V., 2007, Free vibration analysis of functionally graded beams with simply supported edges, *Material Design* **28**(5): 1651–1656.

[8] Gharib A., Salehi M., Fazeli S., 2008, Deflection control of functionally graded material beams with bonded piezoelectric sensors and actuators, *Materials Science and Engineering* **498**: 110-114.

[9] Piovan T., Sampaio R., 2008, Vibrations of axially moving flexible beams made of functionally graded materials, *Thin-Walled Structures* **46**: 112-121.

[10] Xiang H.J., Shi Z.F., 2009, Static analysis for functionally graded piezoelectric actuators or sensors under a combined electro-thermal load, *European Journal of Mechanics A/Solids* **28**: 338-346.

[11] Ying J., Lü C.F., Chen W.Q., 2008, Two-dimensional elasticity solutions for functionally graded beams resting on elastic foundations, *Composite Structures* **84**(3): 209–219.

[12] Sina S.A., Navazi H.M., Haddadpour H., 2009, An analytical method for free vibration analysis of functionally graded beams, *Materials and Design* **30**(3): 741–747.

[13] Simsek M., Kocatürk T., 2009, Free and forced vibration of a functionally graded beam subjected to a concentrated moving harmonic load, *Composite Structures* **90**(4): 465-473.

[14] Simsek M., 2010, Non-linear vibration analysis of a functionally graded Timoshenko beam under action of a moving harmonic load, *Composite Structures* **92**(10): 2532-2546.

[15] Simsek M., 2010, Fundamental frequency analysis of functionally graded beams by using different higher-order beam theories, *Nuclear Engineering and Design* **240**: 697-705.

[16] Khalili S.M.R., Jafari A.A., Eftekhari S.A., 2010, A mixed Ritz-DQ method for forced vibration of functionally graded beams carrying moving loads, *Composite Structures* **92**(10): 2497-2511.

[17] Mahi A., Adda B.E.A., Tounsi A., Mechab I., 2010, An analytical method for temperature-dependent free vibration analysis of functionally graded beams with general boundary conditions, *Composite Structures* **92**(8): 1877-1887.

[18] Craciunescu C.M., Wuttig M., 2003, New ferromagnetic and functionally grade shape memory alloys, *Journal of Optoelectron Advance Material* **5**(1): 139–146.

[19] Fu Y.Q., Du H.J., Zhang S., 2003, Functionally graded TiN/TiNi shape memory alloy films, *Journal of Materials Letters* **57**(20): 2995–2999.

[20] Fu Y.Q., Du H.J., Huang W.M., Zhang S., Hu M., 2004, TiNi-based thin films in MEMS applications: a review, *Journal of Sensors and Actuators A* **112**(2–3): 395–408.

[21] Witvrouw A., Mehta A., 2005, The use of functionally graded poly-SiGe layers for MEMS applications, *Journal of Functionally Graded Materials VIII* **492–493**: 255–260.

[22] Lee Z., Ophus C., Fischer L.M., Nelson-Fitzpatrick N., Westra K.L., Evoy S., et al., 2006, Metallic NEMS components fabricated from nanocomposite Al–Mo films, *Journal of Nanotechnology* **17**(12): 3063–3070.

[23] Rahaeifard M., Kahrobaiyan M.H., Ahmadian M.T., 2009, Sensitivity analysis of atomic force microscope cantilever made of functionally graded materials, *Proceedings of the 3rd international conference on micro-and nanosystems (MNS3)*, San Diego, CA, USA.

[24] Senturia S., 2001, *Microsystem Design*, Norwell, MA: Kluwer.

[25] Sadeghian H., Rezazadeh G., Osterberg P., 2007, Application of the generalized differential quadrature method to the Study of Pull-In Phenomena of MEMS switches, *Journal of Micro Electromechanical System IEEE/ASME* **16**(6): 1334-1340.

[26] Rezazadeh G., Khatami F., Tahmasebi A., 2007, Investigation of the torsion and bending effects on static stability of electrostatic torsional micromirrors, *Journal of Microsystem Technologies* **13**(7): 715-722.

[27] Sazonova V., 2006, *A Tunable Carbon Nanotube Resonator*, Ph.D. Thesis, Cornell University.
[28] Rezazadeh G., Tahmasebi A., Zubtsov M., 2006, Application of piezoelectric layers in electrostatic MEM actuators: controlling of Pull-in Voltage, *Journal of Microsystem Technologies* **12**(12): 1163-1170.
[29] Bao M., Wang W., 1996, Future of Micro Electromechanical Systems (MEMS), *Sensors and Actuators A: Physical* **56**: 135-141.
[30] Mehdaoui A., Pisani M.B., Tsamados D., Casset F., Ancey P., Ionescu A.M., 2007, MEMS tunable capacitors with fragmented electrodes and rotational electro-thermal drive, *Journal of Microsystem Technologies* **13**(11): 1589-1594.
[31] Zhang Y., Zhao Y., 2006, Numerical and analytical study on the pull-in instability of micro- structure under electrostatic loading, *Journal of Sensors and Actuators A: Physical* **127**: 366-367.
[32] Nguyen C.T.C., Katehi L.P.B., Rebeiz G.M., 1998, Micromachined devices for wireless communications, *Proceedings of the IEEE* **86**(8): 1756-1768.
[33] Hasanyan D.J., Batra R.C., Harutyunyan S., 2008, Pull-in instabilities in functionally graded micro-thermo electromechanical systems, *Journal of Thermal Stresses* **31**: 1006–1021.
[34] Jia X.L., Yang J., Kitipornchai S., 2010, Characterization of FGM micro-switches under electrostatic and Casimir forces, *Materials Science and Engineering* **10**: 012178.
[35] Zhou L., Tang D., 2007, A functionally graded structural design of mirrors for reducing their thermal deformations in high-power laser systems by finite element method, *Optics & Laser Technology* **39**: 980–986.
[36] Noda N., Jin Z.J., 1993, Steady thermal stresses in an infinite nonhomogenous elastic solid containing a crack, *Thermal Stresses* **16**: 116–181.
[37] Erdogan F., Wu B.H., 1996, Crack problems in FGM layers under thermal stresses, *Journal of Thermal Stresses* **19**: 237–265.
[38] Asghari M., Ahmadian M.T., Kahrobaiyan M.H., Rahaeifard M., 2010, On the size-dependent behavior of functionally graded micro-beams, *Journal of Materials and Design* **31**: 2324–2329.
[39] Martin H., 2009, *Sadd, Elasticity, Theory, Applications, and Numerics*, Academic Press, second Edition.
[40] Mohammadi-Alasti B., Rezazadeh G., Borgheei A.M., Minaei S., Habibifar R., 2011, On the mechanical behavior of a functionally graded micro-beam subjected to a thermal moment and nonlinear electrostatic pressure, *Composite Structures* **93**: 1516–1525.
[41] Sun Y., Fang D., Soh A.K., 2006, Thermoelastic damping in micro-beam resonators, *International Journal of Solids and Structures* **43**: 3213-3229.
[42] Younis M., Nayfeh A.H., 2003, A study of the nonlinear response of a resonant micro-beam to an electric actuation, *Journal of Nonlinear Dynamics* **31**: 91–117.
[43] Neubrand A., Chung T.J., Steffler E.D., Fett T., Rodel J., 2002, Residual stress in functionally graded plates, *Journal of Material Research* **17**(11): 2912–2920.
[44] Bin J., Wanji C., 2010, A new analytical solution of pure bending beam in couple stress elasto-plasticity, Theory and applications, *International Journal of Solids and Structures* **47**: 779–785.
[45] Abbasnejad B., Rezazadeh G., 2012, Mechanical behavior of a FGM micro-beam subjected to a nonlinear electrostatic pressure, *International Journal of Mechanics and Materials in Design*, 8:381–392 .
[46] Rezazadeh G., Pashapour M., Abdolkarimzadeh F., 2011, Mechanical behavior of a bilayer cantilever microbeam subjected to electrostatic force, mechanical shock and thermal moment, *International Journal of Applied Mechanics*, **3**(3): 543–561.
[47] Rezazadeh G., Fathalilou M., 2011, Pull-in Voltage of electrostatically-actuated microbeams in terms of lumped model Pull-in Voltage using novel design corrective coefficients, sensing and imaging, *An International Journal* **12**(3-4):117-131.
[48] Bhangale R.K., Ganesan N., Padmanabhan C., 2006, Linear thermoelastic buckling and free vibration behavior of functionally graded truncated conical shells, *Journal of Sound and Vibration* **292**: 341–371.
[49] Yang J., Liew K.M., Wu Y.F., Kitipornchai S., 2006, Thermo-mechanical post-buckling of FGM cylindrical panels with temperature-dependent properties, *International Journal of Solids Structures* **43**: 307–324.
[50] Ke L.L., Yang J., Kitipornchai S., 2010, Nonlinear free vibration of functionally graded carbon nanotube-reinforced composite beams, *Composite Structures* **92**: 676–683.
[51] Alibeigloo A., 2010, Thermoelasticity analysis of functionally graded beam with integrated surface piezoelectric layers, *Composite Structures* **92**: 1535–1543.
[52] Anandakumar G., Kim J.H., 2010, On the modal behavior of a three-dimensional functionally graded cantilever beam: Poisson's ratio and material sampling effects, *Composite Structures* **92**: 1358–1371.
[53] Azizi S., 2008, Design of micro accelerometer to use as airbag activator, MSc thesis, Mechanical Engineering Department, Tarbiat Modares University, Tehran, Iran, 53–54, (in Persian).
[54] Seydel R., 2009, *Practical Bifurcation and Stability Analysis*, Springer-Verlag New York, LLC, Third Edition.
[55] Kuznetsov Y.A., 1998, *Elements of Applied Bifurcation Theory*, Springer-Verlag, New York, Second Edition.